Ingeniería 16 (2): 55-62, ISSN: 1409-2441; 2006. San José, Costa Rica

CENTRIFUGAL FAN IMPELLER FAILURE ANALYSIS USING FINITE ELEMENTS

Juan Gabriel Monge Gapper

Abstract

This article shows the failure analysis assisted with finite element modeling of a centrifugal fan impeller that was originally part of the burner of a 1175 kW [120 bhp] saturated steam boiler. The linear stress and vibration modes model pointed to the origin of the apparently sudden failure.

Keywords: centrifugal fan, fan model, modal analysis, resonance failure, finite elements.

Resumen

Este artículo es un análisis de falla ayudado por el modelado matemático de un rodete de un abanico centrífugo que formaba parte del quemador de una caldera de vapor saturado con una capacidad nominal de 1175 kW [120 cv]. El modelado de esfuerzos lineal y de los modos de vibración permitió delimitar el origen de la falla aparentemente repentina del rodete.

Palabras clave: ventilador centrífugo, modelo de rodete, análisis modal, falla por resonancia, elementos finitos.

Received: 06 March 2005 • **Accepted:** 18 January 2007

1. INTRODUCTION

This case study originally was requested to determine the cause of the sudden structural failure of the 1500 W [2 hp] single entry centrifugal fan impeller, in order to prevent similar failures in the future.[1] Since this new boiler was under guarantee and had only 760 h of logged operation, the manufacturer replaced the fan impeller at no cost to the facility operators but offered no explanation as to the origin of the problem, which had cost the operator five weeks of downtime.

The failure consisted of the sudden rupture of the middle chassis ring. Although it did not cause a seizure due to a large clearance within the fan housing, the considerable noise and vibration produced led to a manual shutdown of the boiler. The combustion process was apparently unaffected for almost twenty minutes at 20 % load operation before shutdown.

Initial speculations regarding the cause of the failure included corrosion, an unbalanced rotor, a factory-defective rotor, foreign material entering the impeller and sabotage. A faulty structural design and elastic resonance of the rotor were also suggested.

This article does not concentrate exclusively on the Finite element (FE) modeling of the impeller; special emphasis will be given to how rational analysis of many aspects affecting the failure can interact with FE to rule out any unlikely possibilities. FE was used mainly to eliminate rotor resonance and evaluate stress concentration on the outer edge of the middle chassis ring at the failure point, specifically where fabrication notches and blade spaces coincided (see figures 1 and 2), but FE modeling does not point directly to the failure itself.

2. CASE DESCRIPTION

The single-entry impeller was directly coupled to the 1500 W [2 hp] electric motor, operating at 1650 rpm on a single phase 220 V source power. According to boiler specifications, the fan was rated 0,80 m^3/s at 1,50 kPa (1700 ft^3/min at 6 in H_2O). Fan speed is constant at all boiler load conditions: the controller regulates air flow through a servo-driven damper.

The geometry of the impeller (figure 1), about 300 mm in diameter and 150 mm wide consisted of one base disc and two perforated rings to hold forty-eight blades. The disc and rings are pressed from 1 mm (0,05 in) galvanized steel; the backward curved blades are pressed from 0,6 mm (0,025 in) galvanized steel. Four 178 mm [7 in] steel bars (6 mm [0,25 in] in diameter) give the assembly rigidity. Assembly is mechanical, except for the 6 mm bars, which are welded to the outer ring and base disc as shown. The housing had a clearance of about 10 mm [0,5 in] relative to all edges of the impeller.

The failure itself was unfortunately not witnessed by the boiler operator, but probably occurred at low load. As described above, the misshapen impeller did not affect low load operation. The boiler was stopped and the fan disassembled due to high noise and vibration. Figure 2 shows the failed impeller; note how the middle ring failed at the point where a notch and a space for the blade coincided. The secondary failure is the buckling of two of the four support bars.

In addition, there is a layer of rust on all non-galvanized surfaces: all edges, notches and holes were rusted as if the impeller had been in operation for years. The boiler operates at a facility near the sea, with a high relative humidity and occasional salt air. The section of failure deserves special attention: rust covered most of point **a** of failure with no ductile deformation (see figure 2), suggesting a crack that could have been present since manufacture or that could have grown longer during operation of the fan. Failure at point **b** was free of rust and presented typical ductile behavior.

Aside from overheated motor bearings, no other damage was detected in the system. The absence of a protective screen for the entrance of the fan was also noted; however, the impeller showed no traces of binding, scraping or impact.

In this case, it is useful to quantify two aspects that may have led to failure: the relative magnitude of stress at points **a** and **b** *with* and *without* the

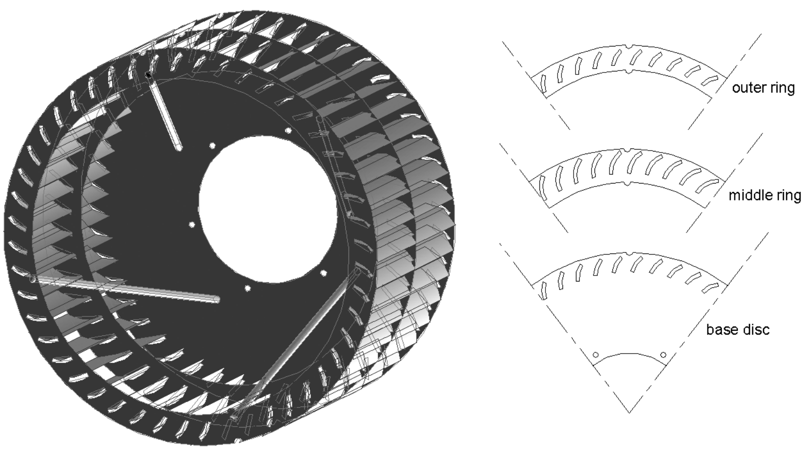

Figure 1. Geometrical configuration of the impeller
Source: (Author)

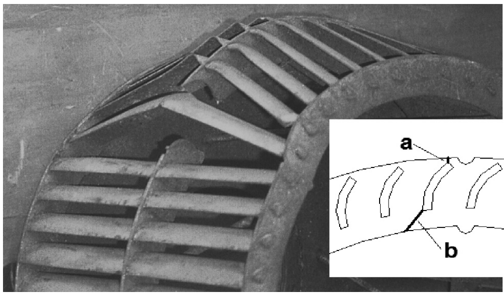

Figure 2. Impeller failed section
Source: (Author)

crack; and the frequency of the natural modes of vibration. Excessively high stresses at **b** would eventually lead to failure, especially considering the fact that it is a rotating -hence vibrating-piece of machinery. On the other hand, any mode of vibration with a frequency near or in phase to that of the rotation can lead to accelerated fatigue at points with stress concentration (such as point **a**).

3. FINITE ELEMENT MODEL AND RESULTS

A single geometrical model of the complete assembly is sufficient for the objectives outlined; a precise reproduction of the failure would require more complex modeling, especially regarding friction between mechanically assembled parts and would not provide further significant information on the problem addressed. The simpler model used here will cover only the elastic behavior of the structure as a whole under the influence of the most important forces present.

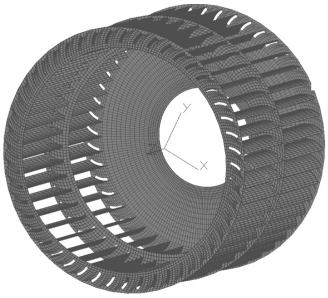

Figure 3. FEA meshing for the impeller[2]
Source: (Author)

The dimensions were taken directly from the failed impeller and reproduced by means of a manually meshed computer model using *Algor®* v. 12,01, as shown in figure 3.

This model implies many simplifications, most of which do not distort results significantly; nevertheless, they must be taken into account while interpreting the results.

Mechanical assemblies. All mechanical assemblies were modeled as solid unions. This would correspond to a completely welded impeller that is more rigid than the real assembly. FE modeling of friction forces is unnecessarily complex for the present case, so this difference must be taken into consideration when interpreting modal analysis results, which are especially sensitive to differences in global elastic behavior.

Pseudo-two-dimensional FE. Both of the rings, the base disc and the blades are essentially two-dimensional objects with an assigned thickness. The finite elements used (plate elements) react to all components of forces and moments, but stresses are constant through the entire thickness. The bars were modeled as tension-compression only elements (truss elements) with a specified cross section.

Existing crack. The possibility of an existing crack at the failure point -identified as **a-** was omitted from the modal analysis, since the crack will not change global elasticity significantly. For stress analysis, two runs were completed—one with the crack and one without—to compare the magnitude of stresses.

Aerodynamic forces. These forces, although necessarily present, are not comparable to centrifugal forces and could be ignored. They are small, with magnitudes along the order of 30 N per blade for the present case according to fan blade calculation procedures outlined by Eck (3). For comparison, centrifugal forces amount to around 850 N per blade. In any case, including these forces would add to the precision of the model, but it would not contribute to the results sought here.

Boundary conditions. The impeller originally was bolted on a cast iron coupling that was considered rigid. Note that although the origin of the forces is dynamic (centrifugal), the finite element model uses the linear static stress equations with the dynamic terms approximated as a constant, as a function of the specified rotational speed.

Other effects. Other effects such as vibration from the motor, an unstable airflow, impeller imbalance, or impact from a foreign object were not included in the present model because they would be of little help and would complicate the finite element model considerably.

Results show relatively low stresses. The areas with the higher values are all found near the union of a blade and a ring due to the chosen modeling of mechanical unions. This distortion does not render the analysis invalid; even if the higher stresses evident in figure 4 were true (Von Mises maximum stress is 57,0 MPa [8270 psi]), they are still lower than the yield stress for many common steels. In fact, the real, less rigid structure will probably present low stresses. The truss elements (bars) all are loaded with low tension stress according to the FE calculations.

To verify this statement, the middle ring was separated and remeshed with a higher density (using the *Algor*® v.12,01 “automatic mesh”), and special forces and boundary conditions were used as well. In this case, the centrifugal load from the blades was applied directly as a distributed force acting against the concave portion of all blade support holes. Boundary conditions were applied to some of the innermost finite elements to let the figure displace away from the geometrical center. Rotation speed was specified as before.

Since this middle ring also contained the main failure point, two runs were completed: one with and one without the crack at the first failure point. Figure 5 shows the segment of interest for both cases.

The run executed without the crack shows that the maximum stresses are even lower (311 MPa [4510 psi]) than the equivalent section on the complete assembly. This result is expected; the rigid union with the blade (in the FE model) generates flexure stresses additional to those due to centrifugal forces. Such flexure stresses do not exist when the union is a simple contact, which is the case of the real impeller.

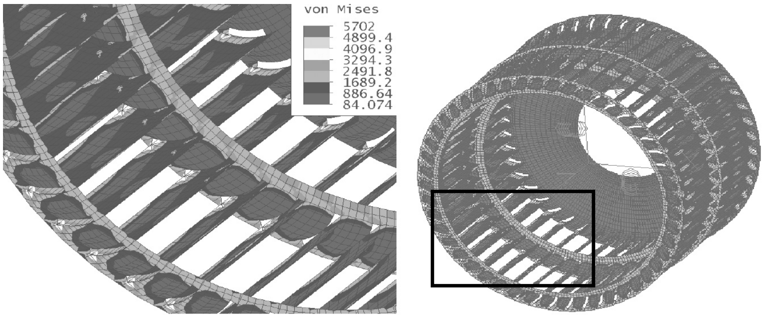

Figure 4. Von Mises stresses for the impeller assembly

Source: (Author)

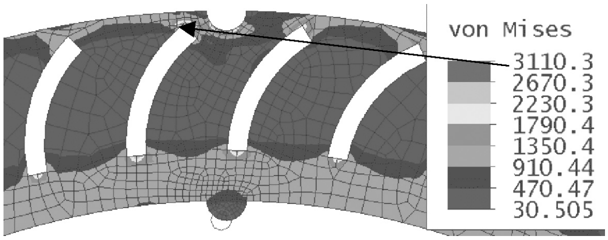

Figure 5a. Von Mises stresses for the middle ring (without a crack)

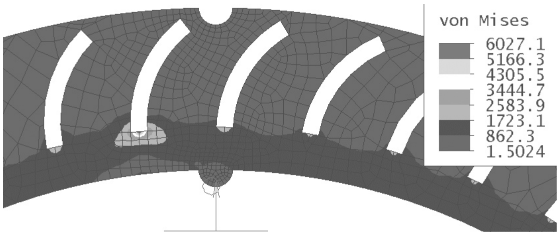

Figure 5b. Von Mises stresses for the middle ring (with a crack)
Source: (Author)

The presence of the crack at point **a** obviously increases the maximum stress, present at the base of the blade hole with the crack. Stresses are almost twice as high, but values still are low at 62,7 MPa [9090 psi].

Finally, modal analysis was performed using *Algor*® 12 with a setup for calculation with fifteen modes of vibration starting at 0 Hz and 40000 Hz as a cutoff frequency. The main modes of vibration were identified between 37,1 Hz and 145 Hz (2226-8700 cpm), and are shown in figure 6.

All other eleven modes either are equivalent variants of the four vibration shapes shown or

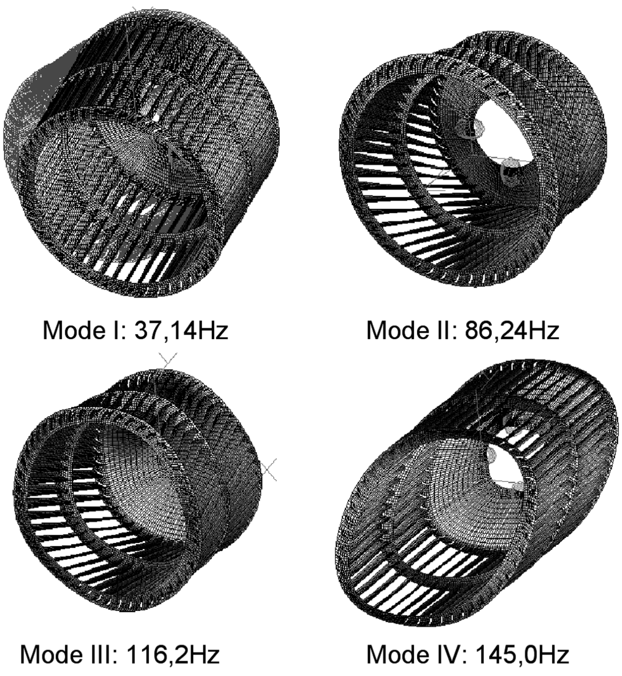

Figure 6. First four main modes of vibration
Source: (Author)

occur at frequencies too high to be of any interest for the present case. None of these frequencies are in phase with the 1650 rpm (27,50 Hz) impeller speed, and only in modes III and IV does important middle ring deformation occur.

4. POSSIBLE CAUSES OF FAILURE

Many causes of failure were speculated on by all parts involved. Those deserving mention will be outlined in this section, while discussing whether the present FE model supports or eliminates these possibilities.

Faulty design. Calculated Von Mises stresses around 31,1 MPa (4510 psi) according to the FE model are quite low in comparison with yield stresses usually around 165-250 MPa [24000-36000 psi] for most commercial steels. With or without the presence of the crack, stresses are low as is usual with most small-diameter fan impellers. Dimensions and selection of materials appear to be appropriate.

Faulty manufacture. The presence of rust at the surface of the failure, low calculated stresses and no plastic deformation at point **a**, suggest that the crack had been present since the boiler was installed. According to calculations, maximum Von Mises stresses would be around 62,7 MPa [9090 psi] and little deflection would occur. The presence of the crack at **a** basically does not affect the operation of the fan unless an additional crack forms at point **b**.

Resonance. The possibility that resonance eventually led to the failure of the middle ring was eliminated. The first mode of vibration (deformation of the base disc) takes place at 2226 cycles per minute, and the fan operates at 1650 rpm. Rotor imbalance also would lead to the deformation of the base disc similar to that of Mode I, but would not be related to middle ring failure, so this possibility also can be ruled out.

Impact. The FE model is of no help in this case, but certainly a large enough object could have hit the inside of the middle ring at point **b** and caused the rupture if point **a** had already failed. The layer of dust and grime that normally accumulates on impellers had no sign of scraping or impact with sharp objects.

Corrosion. Since none of the edges were galvanized, corrosion had built up noticeably on all of them, including of course the blade spaces on the middle ring. The accelerated corrosion near zones with a high stress concentration could have caused a crack to form and grow at point b, starting at the inside of the blade spaces where the higher stresses appear (see figure 5b). Normal vibration could have contributed to failure, but not necessarily be the origin.

In addition, it is important to note that the new impeller has an identical geometrical configuration, was properly balanced and has no visible cracks at the critical sections. It was also spray-painted with two coats of anticorrosive paint. After more than 6500 h of operation, there have been no other problems related to the fan.

5. CONCLUSIONS

From the FE modeling results and the initial conditions described in section 2, the following statements can be made regarding the failure of the fan:

1. The mechanical design was not faulty. All parts of the assembly have a safety factor of at least 3, even with a single crack on the outer rim of the middle ring.

2. Resonance was not the cause of failure; both imbalance and the lower frequencies of vibration have no relation with excessive stress on the middle ring. In any case, all modes of vibration occur at frequencies higher than the rotation speed.

3. Failure is imminent once the outer point **a** is damaged enough to transfer stress concentration to the inner point **b**. Such stress concentration accelerates any corrosion

process, which finally overstresses point **b** to the point of failure.

4. Once there was a small gap at failure point **a** with all stresses concentrated on point **b**, overall failure was gradual, and evolved over the course of a few days. Corrosion could have initiated or accelerated failure of point **a**, and it could have been present since the fan was new. Point **b** evolved similarly: corrosion, accelerated by high stresses, led to the formation and growth of a crack that further stressed the remaining material and ended with a sudden rupture.

5. The fan continued operating since the misshapen impeller did not lose any pieces or bind with the housing. The airflow was reduced, but not interrupted since most of the blades were still close to their original position; and because the boiler was on a period of low demand, the controller did not detect the irregular condition.

6. Buckling of two of the four support bars probably occurred after the middle ring failure. It can be shown (and proven mathematically or with a finite analysis model) that compression forces on these bars are impossible unless there is resonance or if the assembly has lost its symmetry. (Ugural & Fenster, 2000) addresses similar problems on the chapter on axisymmetrically loaded objects. Vibration modes such as those calculated could lead to buckling of the bars, but the buckled bars would not contribute to a failure at point **a**.

7. Stress concentration factors in the impeller assembly can be as high as 6 due to the presence of blade spaces and certain notches on the middle ring. The effect of both could be attenuated with simple modifications to the original design.

Unlike other work on problem-solving through FE modeling (such as Kelecy, 2006 (4)), building an extremely realistic model was not our objective; here the model was built with just enough detail to provide insight on the behavior of the impeller. However, those results were just as important as physical observations and as any rational or intuitive hypothesis regarding the evolution of the failure. In this case, no matter how detailed the FE model, corrosion would have not been pointed out as the cause of the problem. FE modeling is an extremely powerful tool, but as such, is no substitute for insight or a proper problem-solving strategy. Software will continue to evolve, but only thanks to the evolution of insight on everyday engineering problems.

NOTES

1. The names of the companies and people involved are not disclosed due to the publication agreements for the present article.

2. The four rigidizing bars appear as single lines, and are not visible in this image.

BIBLIOGRAPHY

Algor, I. (2001). Algor Finite Element Analysis Software, v. 12.01.

Cook, R. & Others (1989). Concepts and applications of finite element analysis. Third edition. New York:John Wiley and Sons.

Eck, B. (1973) Fans: Design and Operation. Oxford: Pergamon Press.

Kelecy, F. (2006). “Study Demonstrates that Simulation Can Accurately Predict Fan Performance”. Journal Articles by fluent software users. Online article (ja108.pdf) January 2006. http:// www.fluent.com. January the 8th.

Kohan, A. (2000). Manual de Calderas. Madrid: McGraw-Hill.

Reddy, J. N. & Gartling, D. K. (2001). The Finite Element Method in Heat Transfer and Fluid Dynamics. Second edition. Boca Raton: CRC. Press.

Shigley, J. E. & Mischke. (2000). Standard Handbook of Machine Design. New York: McGraw-Hill.

Ugural, A & Fenster, S. (1995). Advanced Strength and Applied Elasticity. Third edition. New Jersey: Prentice Hall.

ABOUT THE AUTHOR

Juan Gabriel Monge Gapper

Master in Mechanical Engineering.

School of Mechanical Engineering, the Universty of Costa Rica.

Phone: 207-5696

Fax: 207-5610

P. O. Box: 10609-1000 San José, Costa Rica.

E-mail: gmonge@fing.ucr.ac.cr